

$SU(N)$ geometries and topological string amplitudes

Amer Iqbal¹ and Amir-Kian Kashani-Poor²

¹Jefferson Laboratory, Harvard University, Cambridge, MA 02138, USA

²Department of Physics and SLAC, Stanford University, Stanford,
CA 94305/94309, USA

Abstract

It has been conjectured recently that the field theory limit of the topological string partition functions, including all higher genus contributions, for the family of CY3-folds giving rise to $\mathcal{N} = 2$ 4D $SU(N)$ gauge theory via geometric engineering can be obtained from gauge instanton calculus. We verify this surprising conjecture by calculating the partition functions for such local CYs using diagrammatic techniques inspired by geometric transitions. Determining the Gopakumar–Vafa invariants for these geometries to all orders in the fiber wrappings allows us to take the field theory limit.

1 Introduction

Topological string theory has received much attention recently due to its implications for large N dualities in the physical string theory [1]. The amplitudes of the topological string theory not only have mathematical significance as generating functions of Gromov–Witten invariants but also

compute coefficients of certain F-terms in the physical 4d theory. Much progress has been made toward their calculation for local toric CY3-folds in the past year [2–5].

In this paper, we will compute the topological string partition function $F = \sum F_g g_s^{2g-2}$ for local Calabi–Yau 3-folds which are resolved A_n singularities fibered over \mathbb{P}^1 . These geometries are used to geometrically engineer $\mathcal{N} = 2$ $D = 4$ $SU(N)$ theories [6–9]. Our interest in these theories stems from the following recent developments in instanton calculus [10–12]. The problem of computing the gauge instanton coefficients \mathcal{F}_k was reduced to the solution of certain integrals over the (reduced) instanton moduli space in [13–18]. These integrals prove difficult to solve for $k \geq 2$. Nekrasov [10] performs a deformation of the integrand which allows their evaluation. The deformed integrals are then assembled into a generating function, the expression for which is computed in [10–12], and the \mathcal{F}_k can be extracted from this expression. The surprising conjecture in [10] is that this generating function itself has an interpretation: it represents the field theory limit of the topological string partition function on the local CY which geometrically engineers the gauge theory. The deformation parameter here plays the role of the string coupling. Inspired by the form of this expression, [10] also contains a conjecture about the form of the full string partition function, before taking the field theory limit. It is these two conjectures, the interpretation of the generating function and the form of the full string partition function, which we wish to investigate, and which we verify, the latter for a certain choice of fibration of the geometry, in this paper.

Specifically, the form of the topological string partition function conjectured in [10] is

$$Z_{\text{Nekrasov}} := \sum_{R_1, \dots, R_N} \varphi^{l_{R_1} + \dots + l_{R_N}} \prod_{l, n=1}^N \prod_{i, j=1}^{\infty} \frac{\sinh[\beta(a_{ln} + \hbar(\mu_{l,i} - \mu_{n,i} + j - i))/2]}{\sinh[\beta(a_{ln} + \hbar(j - i))/2]}. \quad (1.1)$$

This turns out to be the topological string partition function of the distinguished fibration of resolved A_{N-1} over \mathbb{P}^1 which is an orbifold of the resolved conifold. The expression we obtain in this paper for this case is

$$\hat{Z} = \sum_{R_1, \dots, R_N} \varphi^{l_1 + \dots + l_N} \frac{\prod_{i=1}^N \mathcal{W}_{R_i}(q)^2}{\prod_{1 \leq i < j \leq N} \prod_k (1 - q^k Q_i \dots Q_{j-1})^{2C_k(R_i, R_j^T)}, \quad (1.2)$$

where φ is a combination of Kähler parameters. We demonstrate the equivalence of these two expressions in Section 5 of this paper.

The technique we use to calculate the string partition function is inspired by [2]. There, it is shown how to pass to an open string geometry dual

to the closed geometry, on which the partition function can be calculated using Chern–Simons theory. In [4], diagrammatic rules are extracted from this procedure for a subclass of geometries which allow the calculation to proceed without knowledge of the open string geometry. These rules have been completed and given a physical interpretation in the recent paper [5].

To perform the calculation of the string partition function in the case at hand, a further hurdle must be overcome. The expression obtained by [10–12] and the one conjectured by [10] translate into topological string theory expressions which are an expansion in wrappings of the base \mathbb{P}^1 but *exact* in fiber wrappings. We show how to obtain these exact results by making an assumption about the form of an expression which enters in the Chern–Simons calculation, generalizing an approach utilized in [19].

The plan of the paper is as follows. In Section 2, we briefly review how $\mathcal{N} = 2$ $SU(N)$ gauge theories in $D = 4$ are engineered in string theory. Section 3 explains the diagrammatic techniques we employ to perform our calculation, and their origins. In Section 4, we introduce the final ingredient of our calculation which allows the determining of the integral invariants to all orders in fiber wrappings, perform the calculation for $SU(3)$ geometries in detail, and show how the result generalizes to $SU(N)$. In the final section, we compare our results to those obtained based on gauge instanton calculus. In Appendix A, we provide some details on the geometries studied in this paper and their toric description, and make some comments relating to the $5d$ theory one obtains by considering M-theory on these CY geometries.

2 Geometric engineering of $SU(N)$ theories

Compactifications of type IIA on singular CYs yield effective four-dimensional theories with enhanced gauge symmetry [6–8]. The gauge symmetry in the field theory arises from D2-branes wrapping collapsing curves in the CY3-fold. Thus to get a particular gauge symmetry, one has to study a CY3-fold with the appropriate shrinking cycles.

The engineering of an $SU(N)$ gauge theory requires a singularity of A_{N-1} type. Type IIA compactification on such a geometry gives a six-dimensional $SU(N)$ theory with sixteen supercharges. To obtain a four-dimensional theory, further compactification on a two-dimensional surface is required. If the four-dimensional surface is T^2 , the four-dimensional theory acquires $\mathcal{N} = 4$ supersymmetry. To break supersymmetry down to $\mathcal{N} = 2$ (eight supercharges), the surface should have no holomorphic one forms and therefore has to be a \mathbb{P}^1 . To obtain a CY3-fold, the A_{N-1} must be fibered

non-trivially over the \mathbb{P}^1 . The web diagram corresponding to such a geometry is given in figure 1. We review aspects of such geometries in Appendix A. The details of the $\mathcal{N} = 2$ theory obtained by type IIA compactification on such a CY3-fold depend on the choice of fibration. In the field theory limit, which we review next, all such 3-folds reduce to the same theory.

The field theory limit is obtained by taking the string scale to infinity. By the relations of the base and fiber Kähler parameters to the gauge coupling and W-boson masses, these parameters must be scaled as¹

$$Q_B := e^{-T_B} = \left(\frac{\beta\Lambda}{2}\right)^{2N}, \quad Q_{F_i} := e^{-T_{F_i}} = e^{-\beta a_{i,i+1}} \quad i = 1, \dots, N-1. \quad (2.1)$$

Λ above denotes the quantum scale in four dimensions, the $a_{i,i+1} = a_{i+1} - a_i$ parameterize the VEVs of adjoint scalars in the Cartan subalgebra of the gauge group, and the parameter β is introduced such that the field theory limit corresponds to $\beta \rightarrow 0$.

The $\mathcal{N} = 2$ prepotential has both 1-loop perturbative and non-perturbative (instanton) contributions,

$$\mathcal{F} = \mathcal{F}_{\text{classical}} + \mathcal{F}_{1\text{-loop}} + \sum_{k=1}^{\infty} c_k(a_i) \Lambda^{2Nk}. \quad (2.2)$$

We compare this to the expansion of the genus zero topological string amplitude

$$F_0(T_B, \{T_{F_i}\}) = P_3(T_B, \{T_{F_i}\}) + \sum_{(k,\mathbf{m}) \neq (0,0)} \sum_{n=1}^{\infty} \frac{N^{0(k,\mathbf{m})}}{n^3} e^{-nkT_B - n \sum_i m_i T_{F_i}}, \quad (2.3)$$

(here $P_3(T_B, \{T_{F_i}\})$ is a cubic polynomial from which one gets the classical contribution to the prepotential). The contributions of worldsheet instanton multiwrappings, $n > 1$, vanish in the field theory limit. By considering (2.1), it then becomes clear that the k -th gauge instanton contributions stem from worldsheet instantons that wrap the base \mathbb{P}^1 of our geometries k -times.

In this paper, we will be interested in taking the field theory limit of the full topological partition function $\sum g_s^{2g-2} F_g$, rather than just studying the genus 0 contribution. We are motivated to study the full quantity due to recent works [10–12] which obtain it, as reviewed in Section 5, via instanton calculations within field theory. Obtaining finite contributions from all genera requires scaling the string coupling such that $q := e^{ig_s} = e^{\beta\hbar} \cdot \hbar$ will

¹In the following, the notation Q_c will always be reserved for the exponential of minus the corresponding Kähler parameter, e^{-T_c} .

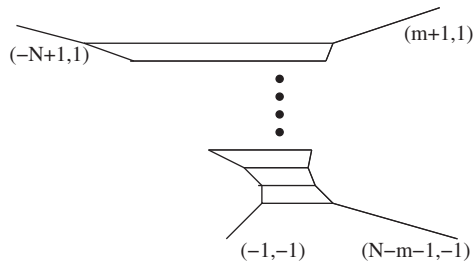


Figure 1: The web diagram for $SU(N)$ geometries. The tuples in parentheses signify the slope of the respective lines.

serve to distinguish between the contributions at different g_s (the notation is chosen in accordance with [10]).

3 Diagrammatics

3.1 Geometric transitions

In [20], the string theory partition function $\sum g_s^{2g-2} F_g$ is shown to have the following form

$$\sum_{g=0}^{\infty} g_s^{2g-2} F_g(\omega) = \sum_{\Sigma \in H_2(X)} \sum_{g=0}^{\infty} \sum_{n=1}^{\infty} \frac{N_{\Sigma}^g}{n} \left(2 \sin \left(n \frac{g_s}{2} \right) \right)^{2g-2} e^{-n\Sigma \cdot \omega}. \quad (3.1)$$

In [2], the Gopakumar–Vafa invariants N_{Σ}^g for a given local Calabi–Yau are determined by using duality to the open topological string on a deformed geometry obtained by performing local conifold transitions. The worldsheet instantons of this deformed geometry are under strict control, and by [21], Chern–Simons theory can be used to determine the open string partition function. In particular, open string worldsheet instantons map the boundaries of the worldsheet to S^3 's in the target space, and their contribution to the partition function is captured within the Chern–Simons theory by Wilson loops on the image of these boundaries. For this paper, we will require the expression $W_{R_1 R_2}$ for the expectation value of two Wilson loops in representations R_1, R_2 of $SU(N)$ on an S^3 forming a Hopf link. This is given by²

$$W_{R_1 R_2} = \dim_q R_1 (\lambda q)^{l_2/2} s_{\mu^2}(E_{\mu^1}(t)). \quad (3.2)$$

²For a derivation of the following expressions for Wilson loop amplitudes in Chern–Simons theory, the reader is referred to [22] and references cited therein.

Here, q is the exponential of the Chern–Simons coupling, $q = \exp(\frac{2\pi i}{k+N})$, λ the exponential of the 't Hooft coupling, $\lambda = q^N$. $\mu^{1,2}$ denote the Young tableaux corresponding to the representations R_1, R_2 . $\dim_q R$, the quantum dimension of the representation R , is the normalized expectation value of a Wilson loop in representation R on an unknot, given by

$$\dim_q R = \prod_{1 \leq i < j \leq d} \frac{[\mu_i - \mu_j + j - i]}{[j - i]} \prod_{i=1}^d \prod_{v=1}^{\mu_i} \frac{[v]_\lambda}{[v - i + d]}, \quad (3.3)$$

where $[x]_\lambda = \lambda^{1/2} q^{x/2} - \lambda^{-1/2} q^{-x/2}$, $[x] = [x]_1$, d denotes the number of rows in the tableau μ and μ_i denotes the number of boxes in the i -th row of μ . Finally, s_μ is the Schur polynomial of the representation described by μ , given by

$$s_\mu = \det M_\mu, \quad (3.4)$$

where the $r \times r$ matrix M_μ , with r the number of columns in μ , is given by $M_\mu^{(ij)} = (a_{\mu_i^\vee + j - i})$. μ^\vee is the transposed Young tableaux to μ , obtained by interchanging columns and rows. The a_i are the coefficients of the power series which is the argument of the Schur polynomial, in our case the coefficients of t^i in the expansion of E_μ , given by

$$E_\mu(t) = \left(1 + \sum_{n=1}^{\infty} \left(\prod_{i=1}^n \frac{1 - \lambda^{-1} q^{i-1}}{q^i - 1} \right) t^n \right) \left(\prod_{j=1}^d \frac{1 + q^{\mu_j - j} t}{1 + q^{-j} t} \right). \quad (3.5)$$

The open string parameters q and λ map to the closed string parameters e^{ig_s} and e^t , where t is the Kähler parameter of the compact curve obtained by resolving the conifold singularity (note that q and λ are not independent parameters, whereas g_s and t are). Upon rewriting the Chern–Simons amplitude in terms of closed string parameters, one obtains all Gopakumar–Vafa invariants N_Σ^g up to a given degree in Σ .

The open geometry related via flops and blowdowns to the $SU(3)$ geometry is depicted in figure 2.³ As we describe in the next subsection, it is not necessary to compute the complete open string partition function and then take appropriate limits to arrive at the desired closed string result. A shortcut is available.

3.2 The emergence of diagrammatic rules

Upon calculating closed topological amplitudes using geometric transitions and CS theory, it was noticed by several authors [2, 4, 5] that diagrammatic

³For a more detailed description of such transitions and an explanation of diagrams such as figure 2, see e.g., [19].

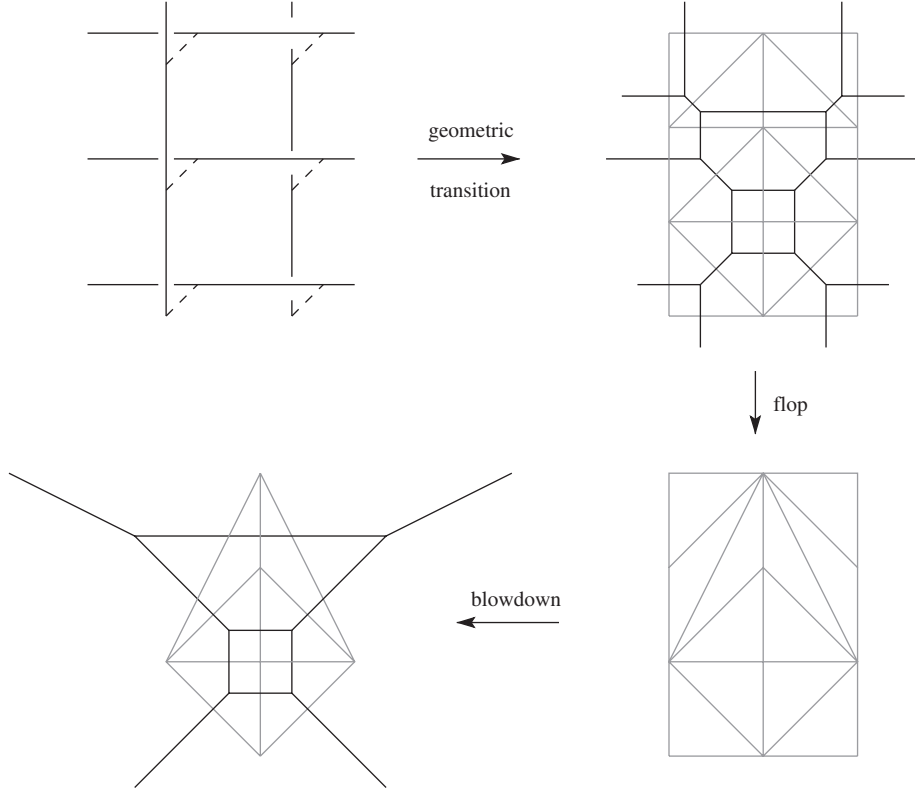


Figure 2: The open geometry dual to a resolved A_2 over \mathbb{P}^1 fibration.

rules emerge which allow writing down the amplitude by considering the web diagram of the closed string geometry. All internal lines are labeled by representations of $SU(N)$, which must be summed over. They contribute factors $Q_c^l = e^{-lT_c}$ to the amplitude, where T_c is the Kähler class of the curve represented by the internal line, and l is the length of the representation. Vertices with two internal lines carry a factor \mathcal{W}_{R_1, R_2} , which is the leading order contribution in λ to the quantity $W_{R_1 R_2}$ introduced in (3.2) above,

$$\mathcal{W}_{R_1 R_2}(q) = \mathcal{W}_{R_1}(q) q^{l_{R_2}/2} s_{\mu_{R_2}}(\mathcal{E}_{\mu_{R_1}}(t)), \quad (3.6)$$

with

$$\mathcal{E}_\mu = \left(1 + \sum_{n=1}^{\infty} \left(\prod_{i=1}^n \frac{1}{q^i - 1} \right) t^n \right) \left(\prod_{j=1}^d \frac{1 + q^{\mu_j - j} t}{1 + q^{-j} t} \right). \quad (3.7)$$

In particular, $\mathcal{W}_R = \mathcal{W}_R$ is given by

$$\mathcal{W}_R(q) = q^{\kappa_R/4} \prod_{1 \leq i < j \leq d} \frac{[\mu_i - \mu_j + j - i]}{[j - i]} \prod_{i=1}^d \prod_{v=1}^{\mu_i} \frac{1}{[v - i + d]}, \quad (3.8)$$

where κ_R is

$$\kappa_R = l_R + \sum_{i=1}^{d(\mu)} \mu_i(\mu_i - 2i). \quad (3.9)$$

These rules are inspired by considering the open string dual to an extended closed geometry, related to the original geometry by blow-ups, such that all internal lines of the original geometry correspond to annulus instantons in the open geometry.⁴ The geometric transition gives rise to additional compact curves, one per local transition from a deformed to a resolved conifold, which are eliminated by taking their Kähler parameters λ_i to infinity. As long as only two annuli end on an S^3 in the open geometry, each S^3 contributes factors $W_{R_1 R_2}$ to the amplitude, and the $\lambda_i \rightarrow \infty$ limit yields the vertex factors $\mathcal{W}_{R_1 R_2}$ as claimed above.

[4] points out the similarity of the diagrammatic rules to Feynman rules, where the Kähler parameters of the 3-fold play the role of Schwinger parameters, the vertices are given by $\mathcal{W}_{R_i R_j}$ and a framing factor described below, and the factor $e^{-l_1 r} \delta_{R_1 R_2}$ can be interpreted as a propagator. This approach has recently been made rigorous in [5].

Let us clarify the diagrammatic approach by looking at two examples.

Consider first the resolved conifold. The relevant amplitude on the open string side here is of course, via the conifold transition, the CS partition function on a sphere. To obtain an expression which adheres to our diagrammatic rules, we follow the seemingly more cumbersome path depicted in figure 3 to arrive at the partition function of the resolved conifold. This is in accordance with the procedure outlined above of relating compact curves of the closed geometry to annulus instantons in the open geometry. Equating the two expressions yields the relation

$$\begin{aligned} \frac{Z}{S_{00}^{-1}(\lambda_1) S_{00}^{-1}(\lambda_2)} &= \lim_{\lambda_1, \lambda_2 \rightarrow \infty} \sum W_{\cdot R}(\lambda_1, q) W_{\cdot R}(\lambda_2, q) \left(\frac{Q}{\sqrt{\lambda_1 \lambda_2}} \right)^{l_R} \\ &\quad (-1)^{l_R} q^{-\kappa_R/2} \\ &= \sum \mathcal{W}_{\cdot R}(q) \mathcal{W}_{\cdot R}(q) Q^{l_R} (-1)^{l_R} q^{-\kappa_R/2} \\ &= S_{00}^{-1}(Q). \end{aligned} \quad (3.10)$$

Note that Q must be renormalized by a factor $\frac{1}{\sqrt{\lambda_1 \lambda_2}}$ in order for the $\lambda_1, \lambda_2 \rightarrow \infty$ limit to exist. Note also that the limit yields the CS partition

⁴Note that this procedure might lead to additional compact divisors, which manifest themselves in the web diagram as crossing external lines.

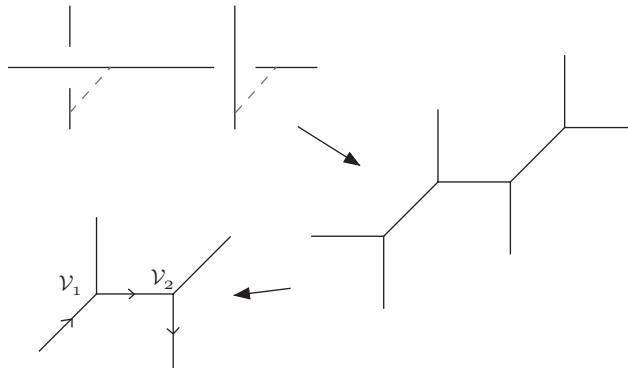


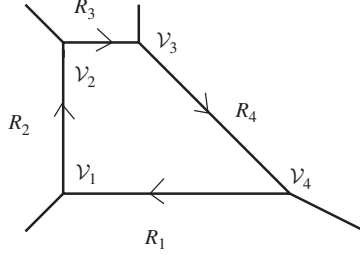
Figure 3: The path to the resolved conifold partition function which yields diagrammatic rules.

function on S^3 proper, not divided by S_{00}^{-1} . Finally, the factor $(-1)^{l_R} q^{-\kappa_R/2}$ is a framing factor. Iqbal [4] proposes the following diagrammatic rules to determine these. Associate with each vertex of the web diagram an $SL(2, \mathbb{Z})$ matrix which maps the (p, q) charge (the slope) of one leg to the (p', q') charge of the other, with (p, q) and (p', q') being the charges associated with two internal legs. In our example, we only have one internal leg at each vertex, so we must think of the bottom diagram in figure 3 as embedded in a larger geometry. The matrix $T^m S^{-1} T^n$ at a vertex $\mathcal{W}_{R_1 R_2}$ gives rise to a framing factor $(-1)^{nl_1 + ml_2} q^{n\kappa_1/2 + m\kappa_2/2}$. For the diagram shown, we obtain the following $SL(2, \mathbb{Z})$ matrices,

$$\mathcal{V}_1 = S^{-1} T^{-1}, \quad \mathcal{V}_2 = S^{-1}, \quad (3.11)$$

in accordance with the framing factor exhibited in (3.10). The expression for $S_{00}^{-1}(Q)$ obtained here will be useful shortly.

The second example we wish to consider is local \mathbb{P}^2 blown up at one point, which is the first del Pezzo surface \mathcal{B}_1 . The web diagram which can be obtained from the toric data is shown in figure 4 below. Again, there are two ways of obtaining the partition function. In [2], see also [3], the geometric transition depicted in figure 5 is considered. Taking the $\lambda_{2,3} \rightarrow \infty$ limit yields a geometry which is related to \mathcal{B}_1 by a flop, see figure 6. In this approach, the Kähler class of the exceptional divisor of the del Pezzo is given by $\log \lambda_1$, i.e., related to the exponential of the Chern–Simons coupling in the open picture. Instead, we can apply the diagrammatic rules outlined above to this example. Here, the Kähler class of the exceptional divisor is related to the renormalized area of the annulus instanton stretching between vertex \mathcal{V}_2 and \mathcal{V}_3 in figure 4.

Figure 4: Web diagram of local \mathbb{P}^2 blown up at one point.

The $SL(2, \mathbb{Z})$ matrices associated to the vertices for this example are given by

$$\nu_1 = S^{-1}, \quad \nu_2 = S^{-1}, \quad \nu_3 = T^{-1}S^{-1}T^{-1}, \quad \nu_4 = TS^{-1}T. \quad (3.12)$$

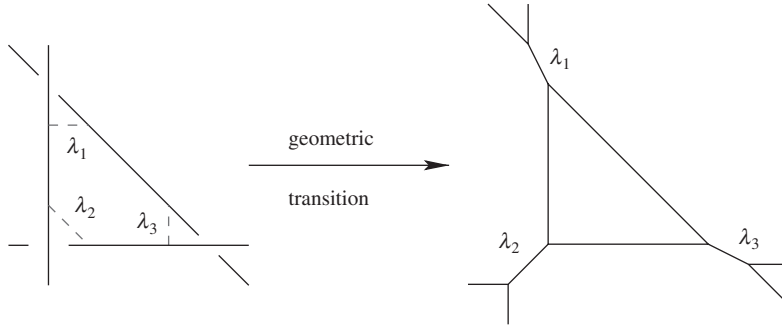
We thus obtain for local \mathcal{B}_1

$$Z = \sum_{R_{1,2,3,4}} Q_B^{l_1+l_3} Q_F^{l_1+l_2+l_4} (-1)^{l_1+l_3} q^{(\kappa_1-\kappa_3)/2} \mathcal{W}_{R_1,R_2} \mathcal{W}_{R_2,R_3} \mathcal{W}_{R_3,R_4} \mathcal{W}_{R_4,R_1}, \quad (3.13)$$

where $T_{B,F}$ are the Kähler parameters of the base and the fiber \mathbb{P}^1 with $Q_{B,F} = e^{-T_{B,F}}$. Note that the expression we obtain from applying diagrammatics only contains $\mathcal{W}_{R_1 R_2}$'s, which are algebraically simpler than the $W_{R_1 R_2}$ that arises in the first approach to this example described above.

Let us define the following generating function of the Gopakumar–Vafa invariants,

$$f_g^{(n)}(x) = \sum_m (-1)^{g-1} N_{(n,m)}^g x^m, \quad (3.14)$$

Figure 5: Obtaining \mathcal{B}_1 via geometric transition and limits.

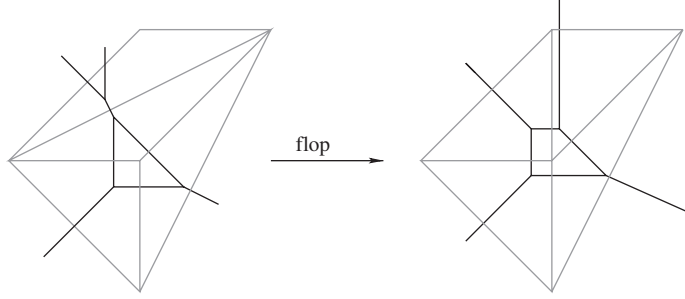


Figure 6: The flop relating the limit of the geometry in figure 5 to \mathcal{B}_1 .

then from (3.13) it follows that

$$\begin{aligned}
 f_g^{(1)}(x) &= \delta_{g,0}(1 + 3x + 5x^2 + 7x^3 + 9x^4 + 11x^5 + 13x^6 + 15x^7 + 17x^8 \\
 &\quad + 19x^9 + 21x^{10} + \dots), \\
 f_0^{(2)}(x) &= 6x^2 + 32x^3 + 110x^4 + 288x^5 + 644x^6 + 1280x^7 + 2340x^8 + 4000x^9 \\
 &\quad + 6490x^{10} + \dots, \\
 f_1^{(2)}(x) &= 9x^3 + 68x^4 + 300x^5 + 988x^6 + 2698x^7 + 6444x^8 + 13916x^9 \\
 &\quad + 27764x^{10} + \dots, \\
 f_2^{(2)}(x) &= 12x^4 + 116x^5 + 628x^6 + 2488x^7 + 836x^8 + 22404x^9 \\
 &\quad + 55836x^{10} + \dots
 \end{aligned}$$

3.3 The three point vertex: $\mathcal{V}_{R_1 R_2 R_3}(q)$

The examples studied above involve open configurations in which at most two annulus instantons end on the same S^3 , or, in terms of diagrammatics, only vertices with at most two internal lines attached occur.

As shown in a recent paper [5], an effective vertex on which three internal lines end (we will refer to this as a three point vertex) can be formulated as well. Once the existence of this vertex is established, the expressions for the vertices V_{R_1, R_2} and V_{\square, R_1, R_2} we will need for our computations can easily be determined as follows.⁵

We consider the subdiagram of a web diagram and its transition, as depicted in figure 7. Assuming the existence of the three point vertex, the

⁵Our vertex differs slightly from [5] in the choice of framing factors.

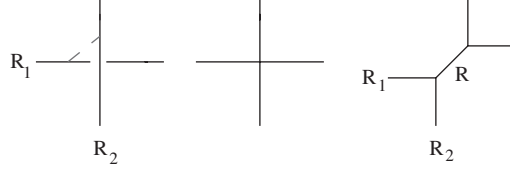


Figure 7: A local transition.

contribution to the partition function coming from the the diagram on the right (RHD) should be given by

$$Z_{R_1 R_2}^{\text{RHD}} = \sum_R Q^{l_R} V_{RR_1 R_2}(q) \mathcal{W}_R(q) (-1)^{l_R} q^{-\kappa_R/2}, \quad (3.15)$$

where the factor of $(-1)^{l_R} q^{-\kappa_R/2}$ is due to the $SL(2, \mathbb{Z})$ transformation, $S^{-1}T^{-1}$, which maps $\begin{pmatrix} 1 \\ 1 \end{pmatrix}$ to $\begin{pmatrix} 1 \\ 0 \end{pmatrix}$.

On the other hand, we know that the diagram on the left (LHD) is given by the CS expectation value of Wilson loops on a Hopf link with the two components in the representations R_1 and R_2 ,

$$Z_{R_1 R_2}^{\text{LHD}} = \lambda^{-(l_{R_1} + l_{R_2})/2} W_{R_1 R_2} \sum_R \lambda^{-l_R} \mathcal{W}_R^2(q) (-1)^{l_R} q^{-\kappa_R/2}. \quad (3.16)$$

In the above expression, $\log \lambda$ is the Kähler parameter of the \mathbb{P}^1 , and $\lambda^{-(l_{R_1} + l_{R_2})/2}$ is the renormalization factor discussed above. Equating (3.15) and (3.16) yields

$$\sum_R Q^{l_R} V_{RR_1 R_2}(q) \mathcal{W}_R(q) (-1)^{l_R} q^{-\kappa_R/2} = \lambda^{-(l_{R_1} + l_{R_2})/2} W_{R_1 R_2} \sum_R \lambda^{-l_R} \mathcal{W}_R^2(q) (-1)^{l_R} q^{-\kappa_R/2}. \quad (3.17)$$

We now set $Q = \lambda^{-1}$ and expand both sides in λ^{-1} to obtain the following expressions for the three point vertex,

$$\begin{aligned} V_{\cdot R_1 R_2} &= \mathcal{W}_{R_1 R_2}, \\ V_{\square R_1 R_2} &= \mathcal{W}_{\square} \mathcal{W}_{R_1 R_2} - \frac{\mathcal{G}_{R_1 R_2}(q)}{\mathcal{W}_{\square}}, \end{aligned} \quad (3.18)$$

where $\mathcal{G}_{R_1 R_2}$ is the next to leading order coefficient in the expansion of $\lambda^{-(l_{R_1} + l_{R_2})/2} W_{R_1 R_2}$,

$$\lambda^{-(l_{R_1} + l_{R_2})/2} W_{R_1 R_2} = \mathcal{W}_{R_1 R_2}(q) + \lambda^{-1} \mathcal{G}_{R_1 R_2}(q) + \dots \quad (3.19)$$

$\mathcal{G}_{R_1 R_2}$ can be determined easily from $W_{R_1 R_2}$,

$$\begin{aligned}\mathcal{G}_{\cdot R}(q) &= -\mathcal{W}_R f_R(q^{-1}), \\ \mathcal{G}_{\square R}(q) &= -\mathcal{W}_R \mathcal{W}_{\square} - \mathcal{W}_{R\square} f_R(q^{-1}),\end{aligned}\tag{3.20}$$

where $f_R(q) = \sum_{i=1}^d \sum_{v=1}^{\mu_i} q^{v-i}$. Thus from (3.18) and (3.20), it follows that

$$V_{\cdot R\square}(q) = \mathcal{W}_{R\square}(q),\tag{3.21}$$

$$\begin{aligned}V_{\square R\cdot}(q) &= \mathcal{W}_{\square} \mathcal{W}_R + \frac{\mathcal{W}_R}{\mathcal{W}_{\square}} f_R(q^{-1}) \\ &= \mathcal{W}_{\square R^T} q^{\kappa_R/2},\end{aligned}\tag{3.22}$$

$$\begin{aligned}V_{\square R\square}(q) &= \mathcal{W}_{\square} \mathcal{W}_{R\square} + \mathcal{W}_R \left(1 + f_R(q^{-1}) \frac{\mathcal{W}_{R\square}}{\mathcal{W}_R \mathcal{W}_{\square}} \right) \\ &= \mathcal{W}_R \left\{ 1 + \frac{\mathcal{W}_{\square R} \mathcal{W}_{\square R^T}}{\mathcal{W}_R \mathcal{W}_{R^T}} \right\},\end{aligned}\tag{3.23}$$

where we have used the following identities,

$$\sum_{i=1}^d \sum_{v=1-i}^{\mu_i-i} q^{-v} = \frac{q}{(q-1)^2} \left\{ \frac{\mathcal{W}_{\square R^T}}{\mathcal{W}_{R^T} \mathcal{W}_{\square}} - 1 \right\},\tag{3.24}$$

$$\mathcal{W}_{R^T}(q) = \mathcal{W}_R(q) q^{-\kappa_R/2},\tag{3.25}$$

$$\frac{\mathcal{W}_{\square R}}{\mathcal{W}_{\square}}(q^{-1}) = -\frac{\mathcal{W}_{\square R}}{\mathcal{W}_{\square}}(q).\tag{3.26}$$

The expression for the vertices given above can be simplified and written as follows

$$\begin{aligned}\frac{V_{\cdot R\square}}{\mathcal{W}_R} &= h_R(q), \\ \frac{V_{\square R\cdot}}{\mathcal{W}_R} &= h_{R^T}(q),\end{aligned}\tag{3.27}$$

$$\frac{V_{\square R\square}(q)}{\mathcal{W}_R} = 1 + h_R(q) h_{R^T}(q),$$

where

$$h_R(q) := \frac{\mathcal{W}_{\square R}}{\mathcal{W}_R} = \mathcal{W}_{\square} + \frac{f_R(q)}{\mathcal{W}_{\square}}.\tag{3.28}$$

4 Calculating the partition function

Using geometric transitions to calculate closed string amplitudes along the lines introduced in [2] computationally involves sums over all representations of $SU(N)$. Aborting the calculation at representations of a certain length,

one obtains the Gopakumar–Vafa invariants $N_{(k,l,\dots)}^g$ for all genera but only up to a restricted level in k, l, \dots .

In [19], we presented a method which, for A_1 fibrations over \mathbb{P}^1 , yields the invariants to all orders in the fiber. This allows us to determine the generating functions

$$f_g^{(k)} = \sum N_{(k,l)}^g Q_F^l, \quad (4.1)$$

where the maximal level k depends on the maximal length of representations we consider. In this section, we will expand the method to A_{N-1} fibrations over \mathbb{P}^1 .

4.1 $SU(2)$

Let us first recall how we proceeded in the case of local Hirzebruch surfaces \mathbb{F}_m , $m = 0, 1, 2$. The relevant CS amplitude is given by [19]

$$\begin{aligned} Z_{\text{CS}}(Q_B, Q_F; q) = \sum_{R_{1,2,3,4}} Q_B^{l_{R_1} + l_{R_3}} Q_F^{m l_{R_1} + l_{R_2} + l_{R_4}} \mathcal{W}_{R_1 R_4}(q) \mathcal{W}_{R_4 R_3}(q) \\ \mathcal{W}_{R_3 R_2}(q) \mathcal{W}_{R_2 R_1}(q) (-1)^{m(l_{R_1} + l_{R_3})} q^{m(\kappa_{R_1} - \kappa_{R_3})/2}. \end{aligned} \quad (4.2)$$

To obtain the exact result to a given order in Q_B , we need to be able to perform the sum

$$K_{R_1 R_2}(Q) = \sum_R Q^{l_R} \mathcal{W}_{R_1 R}(q) \mathcal{W}_{R R_2}(q). \quad (4.3)$$

In the case that R_1 and R_2 are trivial, this expression, $K_{..}(Q)$, has a closed string interpretation: it is the partition function of $T^*(\mathbb{P}^1) \times \mathbb{C}$. This partition function was determined in [2]. It is

$$K_{..}(Q) = \text{Exp} \left\{ \sum_{n=1}^{\infty} \frac{1}{n} \mathcal{W}_{\square}^2(q^n) Q^n \right\}, \quad \mathcal{W}_{\square}(q) = \frac{1}{\sqrt{q} - 1/\sqrt{q}}, \quad (4.4)$$

i.e., $N_m^g = -\delta_{g,0} \delta_{m,1}$. Inspired by this, we parametrize $K_{R_1 R_2}$ for general R_1 and R_2 in the following way,

$$K_{R_1 R_2}(Q) = \mathcal{W}_{R_1}(q) \mathcal{W}_{R_2}(q) \text{Exp} \left\{ \sum_{n=1}^{\infty} \tilde{f}_{R_1 R_2}^n(q) Q^n \right\}. \quad (4.5)$$

The coefficient of the exponential is dictated by comparison of the 0-th order term in Q between (4.3) and (4.5). So far, nothing is gained, since we must

determine the unknown functions \tilde{f}_n for all n . The crucial assumption we now make is that all \tilde{f}_n can be determined from \tilde{f}_1 via

$$\tilde{f}_{R_1 R_2}^n(q) = \frac{\tilde{f}_{R_1 R_2}^1(q^n)}{n}. \quad (4.6)$$

This form for the coefficients of the multicovering is not that surprising since the term in the exponential in this case is a refinement of the open string amplitude which is conjectured [23] to have multicovering contribution with coefficients satisfying the above equation. Once we conjecture this form for $\tilde{f}_{R_1 R_2}^n$, determining $K_{R_1 R_2}(Q)$ is a matter of determining $\tilde{f}_{R_1 R_2}^1$. This can be achieved by expanding (4.3) and (4.5) to first order in Q . A simple calculation yields

$$\begin{aligned} \tilde{f}_{R_1 R_2}^1(q) &= \frac{\mathcal{W}_{R_1 \square} \mathcal{W}_{\square R_2}}{\mathcal{W}_{R_1} \mathcal{W}_{R_2}} \\ &= \frac{q}{(q-1)^2} \left\{ 1 + (q-1) \sum_{j=1}^{d_1} (q^{\mu_j^1 - j} - q^{-j}) \right\} \\ &\quad \left\{ 1 + (q-1) \sum_{j=1}^{d_2} (q^{\mu_j^2 - j} - q^{-j}) \right\}. \end{aligned} \quad (4.7)$$

In the following, it will often be convenient to consider the quantity

$$\hat{K}_{R_1 R_2} = \frac{K_{R_1 R_2}(Q)}{K_{..}(Q)} \quad (4.8)$$

$$= \mathcal{W}_{R_1} \mathcal{W}_{R_2} \text{Exp} \left\{ \sum_n \frac{f_{R_1 R_2}(q^n)}{n} Q^n \right\}. \quad (4.9)$$

The $f_{R_1 R_2}$ are related in a simple way to the $\tilde{f}_{R_1 R_2}$ and the h_R defined in (3.28),

$$f_{R_1 R_2}(q) + \mathcal{W}_{\square}^2(q) = \tilde{f}_{R_1 R_2}^1(q) \quad (4.10)$$

$$= h_{R_1}(q) h_{R_2}(q). \quad (4.11)$$

The coefficients $f_{R_1 R_2}$ were introduced in [19]. They can be written as a finite sum in powers of q and q^{-1} ,

$$f_{R_1 R_2}(q) = \sum_k C_k(R_1, R_2) q^k, \quad (4.12)$$

such that the expansion coefficients have the following properties,

$$\begin{aligned} f_{R_1 R_2}(1) &= \sum_k C_k(R_1, R_2) = l_{R_1} + l_{R_2}, \\ \frac{df_{R_1 R_2}(q)}{dq} \Big|_{q=1} &= \sum_k k C_k(R_1, R_2) = \frac{\kappa_{R_1} + \kappa_{R_2}}{2}. \end{aligned} \quad (4.13)$$

Substituting the expansion (4.12) into (4.8), we obtain

$$\frac{K_{R_1 R_2}(Q)}{K_{..}(Q)} = \mathcal{W}_{R_1} \mathcal{W}_{R_2} \prod_k (1 - q^k Q)^{-C_k(R_1, R_2)}.$$

Thus the partition function of local \mathbb{F}_m is given by

$$\begin{aligned} Z(Q_B, Q_F) &= K_{..}^2(Q_F) \sum_{R_{1,2}} (-1)^{m(l_{R_1} + l_{R_2})} q^{m(\kappa_{R_1} - \kappa_{R_2})/2} Q_B^{l_{R_1} + l_{R_2}} Q_F^{m l_{R_1}} \\ &\quad \frac{\mathcal{W}_{R_1}^2 \mathcal{W}_{R_2}^2}{\prod_k (1 - q^k Q_F)^{2C_k(R_1, R_2)}} \\ &= K_{..}^2(Q_F) \sum_{R_{1,2}} Q_B^{l_{R_1} + l_{R_2}} Q_F^{m l_{R_1}} K_{R_1 R_2}(Q_F) K_{R_1 R_2}^{(m)}(Q_F), \end{aligned} \quad (4.14)$$

where we have defined $K_{R_1 R_2}^{(m)}(Q)$ as

$$K_{R_1 R_2}^{(m)}(Q) = (-1)^{m(l_{R_1} + l_{R_2})} q^{m(\kappa_{R_1} - \kappa_{R_2})/2} K_{R_1 R_2}(Q). \quad (4.15)$$

This splitting of $Z(Q_B, Q_F)$ into contributions from K and $K^{(m)}$ can be depicted as in figure 8.

4.2 $SU(3)$

We now consider the case of $SU(3)$ geometries and generalize this to $SU(N)$ in the next subsection. There are four inequivalent geometries giving pure

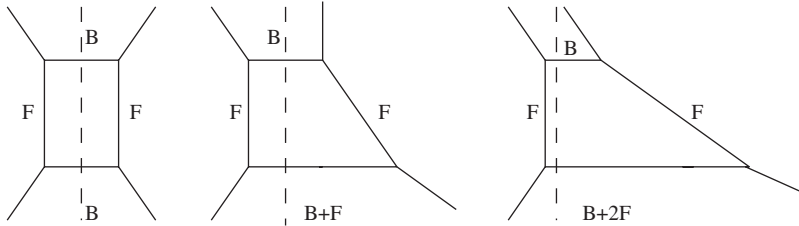


Figure 8: Splitting local \mathbb{F}_m into $K_{R_i R_j}^{(m)}$ contributions.

$SU(3)$ gauge theory via geometric engineering. The web diagram corresponding to these geometries is shown in figure 9. We discuss how these diagrams come about in Appendix A.

Ignoring the angles, these web diagrams all have the ladder structure depicted in figure 10.

The Kähler parameters T_{b_i} are related to the Kähler parameters of the base B and fibers $F_{1,2}$ (recall that $Q_c = e^{-T_c}$) as follows,

$$\begin{aligned} Q_{b_1} &= Q_B Q_{F_1}^{m+1} Q_{F_2}^{(m-1)(1-\delta_{m,0})}, \\ Q_{b_2} &= Q_B Q_{F_2}^{(m-1)(1-\delta_{m,0})}, \\ Q_{b_3} &= Q_B Q_{F_2}^{\delta_{m,0}}. \end{aligned} \tag{4.16}$$

In analogy to the $SU(2)$ case, we split the ladder across its rungs (dashed line in figure 10) and define for each half

$$\begin{aligned} K_{R_1 R_2 R_3}^{(m)}(Q_{F_1}, Q_{F_2}) &= M^{(m)}(q, R_i) \sum_{S_{1,2}} \mathcal{W}_{R_1 S_1}(q) Q_{F_1}^{l_{S_1}} V_{S_1 R_2 S_2}(q) \\ &\quad Q_{F_2}^{l_{S_2}} \mathcal{W}_{S_2 R_3}(q), \end{aligned} \tag{4.17}$$

where $M^{(m)}(q, R_i) = q^{\sum_{i=1}^3 \alpha_i(m) \kappa_{R_i} / 2} (-1)^{\sum_{i=1}^3 \alpha_i(m) l_{R_i}}$ is a framing factor. The Q_{F_1, F_2} independent term in the above expression is given by $K_{R_1 R_2 R_3}^{(m)}(Q_{F_1} = 0, Q_{F_2} = 0) = M^{(m)}(q, R_i) \mathcal{W}_{R_1} \mathcal{W}_{R_2} \mathcal{W}_{R_3}$. We parametrize the Q_{F_1, F_2} dependent pieces as follows

$$\begin{aligned} K_{R_1 R_2 R_3}^{(m)}(Q_{F_1}, Q_{F_2}) &= M^{(m)}(q, R_i) \mathcal{W}_{R_1} \mathcal{W}_{R_2} \mathcal{W}_{R_3} \text{Exp} \left\{ \sum_{n=1}^{\infty} A_{R_1 R_2}^{(n)}(q) Q_{F_1}^n \right. \\ &\quad \left. + \sum_{n=1}^{\infty} A_{R_2 R_3}^{(n)}(q) Q_{F_2}^n + \sum_{n=1}^{\infty} A_{R_1 R_2 R_3}^{(n)}(q) (Q_{F_1} Q_{F_2})^n \right\}. \end{aligned} \tag{4.18}$$

The three sums in the exponential are to take account of the holomorphic curves in the open string geometry and their multicovers running between the upper two, the lower two, and the upper and the lower rung of the

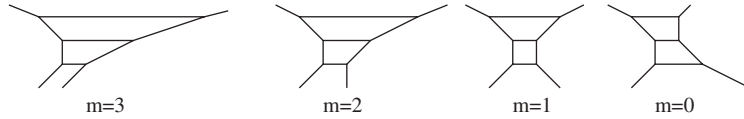


Figure 9: (a) $m = 3$ with \mathbb{F}_2 and \mathbb{F}_4 , (b) $m = 2$ with \mathbb{F}_1 and \mathbb{F}_3 , (c) $m = 1$ with \mathbb{F}_0 and \mathbb{F}_2 , (d) $m = 0$ with \mathbb{F}_1 and \mathbb{F}_1 .

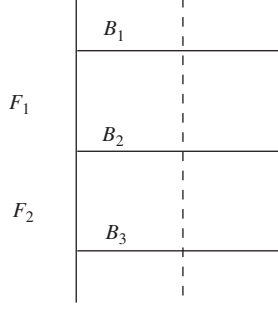


Figure 10: Ladder structure of web diagrams.

ladder. Since this geometry, ignoring the representations on the external legs, is resolved $A_2 \times \mathbb{C}$, holomorphic cycles are in one to one correspondence with positive roots of $SU(3)$, i.e., there are three holomorphic cycles F_1, F_2 and $F_1 + F_2$. Now, we again make an assumption about the coefficient in the multicovering expansion,

$$\begin{aligned} A_{R_1 R_2}^{(n)}(q) &= \frac{A_{R_1 R_2}(q^n)}{n}, & A_{R_2 R_3}^{(n)}(q) &= \frac{A_{R_2 R_3}(q^n)}{n}, \\ A_{R_1 R_2 R_3}^{(n)}(q) &= \frac{A_{R_1 R_2 R_3}(q^n)}{n}. \end{aligned} \quad (4.19)$$

Equating the coefficients of Q_1, Q_2 , and $Q_1 Q_2$ respectively in (4.17) and (4.18) yields

$$\begin{aligned} A_{R_1 R_2}(q) &= \frac{\mathcal{W}_{\square R_1} V_{\square R_2}}{\mathcal{W}_{R_1} \mathcal{W}_{R_2}} \\ &= h_{R_1}(q) h_{R_2^T}(q), \\ A_{R_2 R_3}(q) &= \frac{V_{R_2 \square} \mathcal{W}_{\square R_3}}{\mathcal{W}_{R_2} \mathcal{W}_{R_3}} \\ &= h_{R_2} h_{R_3}, \\ A_{R_1 R_2 R_3} &= \frac{\mathcal{W}_{R_1 \square} V_{\square R_2 \square} \mathcal{W}_{\square R_3}}{\mathcal{W}_{R_1} \mathcal{W}_{R_2} \mathcal{W}_{R_3}} - A_{R_1 R_2} A_{R_2 R_3} \\ &= h_{R_1} h_{R_3}. \end{aligned} \quad (4.20)$$

By (4.10), we hence obtain

$$\begin{aligned} &\hat{K}_{R_1 R_2 R_3}^{(m)}(Q_{F_1}, Q_{F_2}) \\ &:= \frac{K_{R_1 R_2 R_3}^{(m)}(Q_{F_1}, Q_{F_2})}{K_{00}(Q_{F_1}) K_{00}(Q_{F_2}) K_{00}(Q_{F_1} Q_{F_2})} \\ &= \frac{M^{(m)}(q, R_i) \mathcal{W}_{R_1} \mathcal{W}_{R_2} \mathcal{W}_{R_3}}{\prod_k (1 - q^k Q_{F_1})^{C_k(R_1, R_2^T)} (1 - q^k Q_{F_2})^{C_k(R_2, R_3)} (1 - q^k Q_{F_1} Q_{F_2})^{C_k(R_1, R_3)}}. \end{aligned}$$

Define

$$\hat{Z}^{(m)}(Q_{F_1}, Q_{F_2}) := \frac{Z^{(m)}(Q_{F_1}, Q_{F_2})}{K_{00}(Q_{F_1})^2 K_{00}(Q_{F_2})^2 K_{00}(Q_{F_1} Q_{F_2})^2}, \quad (4.21)$$

then

$$\begin{aligned} & \hat{Z}^{(m)}(Q_1, Q_2) \\ &= \sum_{R_{1,2,3}} e^{-T_{b_1} l_{R_1} - T_{b_2} l_{R_2} - T_{b_3} l_{R_3}} \hat{K}_{R_1 R_2 R_3}^{(m_1)}(Q_1, Q_2) \hat{K}_{R_1 R_2 R_3}^{(m_2)}(Q_1, Q_2) \\ &= \sum_{R_{1,2,3}} Q_{b_1}^{l_{R_1}} Q_{b_2}^{l_{R_2}} Q_{b_3}^{l_{R_3}} M^{(m_1)}(q, R_i) M^{(m_2)}(q, R_i) \\ & \quad \frac{\mathcal{W}_{R_1}^2 \mathcal{W}_{R_2}^2 \mathcal{W}_{R_3}^2}{\prod_k (1 - q^k Q_1)^{2C_k(R_1, R_2^T)} (1 - q^k Q_2)^{2C_k(R_2, R_3)} (1 - q^k Q_1 Q_2)^{2C_k(R_1, R_3)}} \\ &= \sum_{R_{1,2,3}} Q_B^{l_1 + l_2 + l_3} Q_{F_1}^{(m+1)l_1} Q_{F_2}^{(m-1)(1-\delta_{m,0})(l_1+l_2) + \delta_{m,0}l_3} \\ & M(q, R_i) \frac{\mathcal{W}_{R_1}^2 \mathcal{W}_{R_2}^2 \mathcal{W}_{R_3}^2}{\prod_{1 \leq i < j \leq 3} \prod_k (1 - q^k Q_{ij})^{2C_k(R_i, R_j^T)}}, \end{aligned} \quad (4.22)$$

where $Q_{12} = Q_{F_1}$, $Q_{23} = Q_{F_2}$, and $Q_{13} = Q_{F_1} Q_{F_2}$. Also in the third line above we have changed R_3 to R_3^T and used (3.25), so that

$$\begin{aligned} M(q, R_i) &= M^{(m_1)}(q, R_i) M^{(m_2)}(q, R_i) q^{-\kappa_3} \\ &= (-1)^{\alpha l_1 + \beta l_2 + \gamma l_3} q^{(\alpha \kappa_1 + \beta \kappa_2 + \gamma \kappa_3)/2}. \end{aligned} \quad (4.23)$$

To determine the framing factors α , β , γ , which of course depend on m , we take $Q_{F_1} \rightarrow 0$, $Q_{F_2} \rightarrow 0$ respectively and thus reduce to the local Hirzebruch geometries we studied in [19] and reviewed in the previous section. To compare the limit of (4.22) to the $SU(2)$ partition function, (4.14), we use (3.25) to rewrite the $SU(3)$ partition function in terms of non-transposed representations. For the geometry containing $\mathbb{F}_k, \mathbb{F}_l$, $(k, l) \neq (1, 1)$, we obtain $\alpha = k$, $\beta = k - 2$ from the $Q_{F_2} \rightarrow 0$ limit and $\beta = l$, $\gamma = l - 2$ from the $Q_{F_1} \rightarrow 0$ limit.⁶ Since k and l are related via $l = k - 2$, we can choose a consistent framing for the full geometry. For the case $(k, l) = (1, 1)$, the $Q_{F_1} \rightarrow 0$ limit yields $\beta = -l$, $\gamma = -l - 2$, again consistent with a choice of framing for the full geometry. In terms of the integer m used to label the $SU(3)$ geometries in figure 9, the framing coefficients are $\alpha = m + 1$, $\beta = m - 1$, $\gamma = m - 3$.

⁶In [19], we consider the local Hirzebruch surfaces \mathbb{F}_k for $k = 0, 1, 2$, since the canonical line bundle over higher Hirzebruch surfaces contains additional compact divisors. Here, we match the $Q_{F_1, F_2} \rightarrow 0$ limit to (4.14) for arbitrary k and show that this allows a consistent choice of framing for all $SU(3)$ geometries.

4.2.1 Gopakumar–Vafa invariants

We can evaluate (4.22) to obtain generating functions for Gopakumar–Vafa invariants,

$$f_g^{(n)}(x, y) = \sum_{k,l} (-1)^{g-1} N_{(n,k,l)}^g x^k y^l. \quad (4.24)$$

We consider the $m = 1$ and $m = 3$ case. The latter was also considered in [5]. For $m = 3$ and $n = 1$, we obtain

$$f_g^{(1)}(x, y) = \delta_{g,0} \left(\frac{y^2}{(1-x)^2(1-y)^2} + \frac{1}{(1-y)^2(1-xy)^2} + \frac{x^4 y^2}{(1-x)^2(1-xy)^2} \right), \quad (4.25)$$

which agrees with [5] upon expansion in x and y . For $n = 2$, the expression for the generating function is too long to reproduce here. It has the form

$$f_g^{(2)}(x, y) = \frac{P_{2,g}(x, y)}{(1-x)^{2g+6}(1-y)^{2g+6}(1-xy)^{2g+6}(1+x)^2(1+y)^2(1+xy)^2}, \quad (4.26)$$

with $P_{2,0}$ a polynomial of order 13 in x , 16 in y , $P_{2,1}$ a polynomial of order 16 in x , 20 in y , etc. We can expand these expressions out to low order in x and y to get

$$\begin{aligned} f_0^{(2)}(x, y) &= 6y^3 + 32y^4 + 110y^5 + (10y^3 + 70y^4 + 270y^5)x + (12y^3 + 96y^4 \\ &\quad + 416y^5)x^2 + (12y^3 + 110y^4 + 518y^5)x^3 + (y^3 + 112y^4 \\ &\quad + 576y^5)x^4 + (14y^3 + 126y^4 + 630y^5)x^5 + \dots \\ f_1^{(2)}(x, y) &= 9y^4 + 68y^5 + (16y^4 + 144y^5)x + (21y^4 + 204y^5)x^2 + (24y^4 \\ &\quad + 248y^5)x^3 + (25y^4 + 276y^5)x^4 + (24y^4 + 288y^5)x^5 + \dots \\ f_2^{(2)}(x, y) &= 12y^5 + 22y^5x + 30y^5x^2 + 36y^5x^3 + 40y^5x^4 + 42y^5x^5 + \dots \end{aligned}$$

For $m = 1$, we obtain

$$f_g^{(1)}(x, y) = \delta_{g,0} \left(\frac{1}{(1-x)^2(1-y)^2} + \frac{1}{(1-y)^2(1-xy)^2} + \frac{x^2}{(1-x)^2(1-xy)^2} \right), \quad (4.27)$$

and

$$\begin{aligned}
 f_0^{(2)}(x, y) &= 6y + 32y^2 + 110y^3 + 288y^4 + 644y^5 + (10y + 70y^2 + 270y^3 \\
 &\quad + 770y^4 + 1820y^5)x + (12y + 96y^2 + 416y^3 + 1280y^4 \\
 &\quad + 3204y^5)x^2 + (6 + 30y + 140y^2 + 560y^3 + 1764y^4 + 4576y^5)x^3 \\
 &\quad + (32 + 98y + 288y^2 + 840y^3 + 2368y^4 + 6020y^5)x^4 \\
 &\quad + (110 + 306y + 672y^2 + 1540y^3 + 3528y^4 + 8064y^5)x^5 + \dots \\
 f_1^{(2)}(x, y) &= 9y^2 + 68y^3 + 300y^4 + 988y^5 + (16y^2 + 144y^3 + 704y^4 \\
 &\quad + 2496y^5)x + (21y^2 + 204y^3 + 1073y^4 + 4032y^5)x^2 + (24y^2 \\
 &\quad + 248y^3 + 1368y^4 + 5368y^5)x^3 + (9 + 16y + 57y^2 + 324y^3 \\
 &\quad + 1653y^4 + 6528y^5)x^4 + (68 + 144y + 252y^2 + 668y^3 \\
 &\quad + 2268y^4 + 7956y^5)x^5 + \dots \\
 f_2^{(2)}(x, y) &= 12y^3 + 116y^4 + 628y^5 + (22y^3 + 242y^4 + 1430y^5)x + (30y^3 \\
 &\quad + 348y^4 + 2168y^5)x^2 + (36y^3 + 434y^4 + 2794y^5)x^3 + (40y^3 \\
 &\quad + 500y^4 + 3308y^5)x^4 + (12 + 22y + 30y^2 + 92y^3 + 616y^4 \\
 &\quad + 3800y^5)x^5 + \dots
 \end{aligned}$$

4.3 $SU(N)$

In this section we generalize the calculation of the previous section to the case of geometries giving rise to $SU(N)$ gauge theory via geometric engineering.

Consider the half-web shown in figure 11 below. Two such webs joined together give rise to the web diagrams for $SU(N)$ geometries depicted in figure 1. As in the case of $SU(3)$ geometries discussed in the last section,

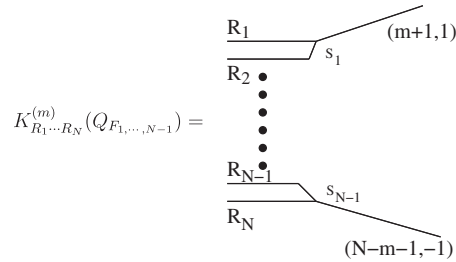


Figure 11: The diagrammatic representation of $K_{R_1 \dots R_N}^{(m)}$. The tuples in parentheses denote the slopes of the corresponding lines.

the partition function associated with such a half-web is given by

$$\begin{aligned}
K_{R_1 \dots R_N}^{(m)}(Q_{F_1, \dots, N-1}) &= M^{(m)}(q, R_i) \sum_{S_1, \dots, N-1} \mathcal{W}_{R_1 S_1}(q) Q_1^{l_{S_1}} V_{S_1 R_2 S_2}(q) \cdots \\
&\quad V_{S_{N-2} R_{N-1} S_{N-1}}(q) Q_{N-1}^{l_{S_{N-1}}} \mathcal{W}_{S_{N-1} R_N}(q) q^{\sum_{i=1}^{N-1} \beta_i \kappa_{S_i}} \\
&\quad (-1)^{\sum_{i=1}^{N-1} \beta_i l_{S_i}}, \tag{4.28}
\end{aligned}$$

where $M^{(m)}(q, R_i) = q^{\sum_{i=1}^N (\alpha_i/2) \kappa_{R_i}} (-1)^{\sum_{i=1}^N \alpha_i l_{R_i}}$. Since the geometry described by the half-web (i.e., ignoring the representations on the external legs) is resolved $A_{N-1} \times \mathbb{C}$, we know that the holomorphic cycles are in one to one correspondence with the positive roots of $SU(N)$ such that the cycles F_i correspond to the simple roots. The above partition function can be written as a sum over all holomorphic curves in the geometry and their multicovering,

$$\begin{aligned}
&K_{R_1 \dots R_N}^{(m)}(Q_{1, \dots, N-1}) \\
&= M^{(m)}(q, R_i) \mathcal{W}_{R_1}(q) \cdots \mathcal{W}_{R_N}(q) \\
&\quad \text{Exp} \left\{ \sum_{i=1}^{N-1} \sum_{r=0}^{N-1-i} \sum_{n=1}^{\infty} A_{R_i \dots R_{i+r+1}}^{(n)}(q) (Q_i Q_{i+1} \cdots Q_{i+r})^n \right\}, \\
&= M^{(m)}(q, R_i) \mathcal{W}_{R_1}(q) \cdots \mathcal{W}_{R_N}(q) \\
&\quad \text{Exp} \left\{ \sum_{i=1}^{N-1} \sum_{r=0}^{N-1-i} \sum_{n=1}^{\infty} \frac{A_{R_i \dots R_{i+r+1}}(q^n)}{n} (Q_i Q_{i+1} \cdots Q_{i+r})^n \right\}, \tag{4.29}
\end{aligned}$$

where, as before, we have assumed

$$A_{R_i \dots R_{i+r+1}}^{(n)}(q) = \frac{A_{R_i \dots R_{i+r+1}}(q^n)}{n}. \tag{4.30}$$

The functions $A_{R_i \dots R_j}(q)$ can be easily determined from (4.29) and (3.28),

$$\begin{aligned}
A_{R_i \dots R_j} &= h_{R_i}(q) h_{R_j^T}(q), \quad j \neq N, \\
A_{R_i \dots R_N} &= h_{R_i}(q) h_{R_N}, \quad i = 1, \dots, N-1.
\end{aligned} \tag{4.31}$$

Define

$$\hat{K}_{R_1 \dots R_N}^{(m)}(Q_1, \dots, Q_{N-1}) = \frac{K_{R_1 \dots R_N}^{(m)}}{\prod_{1 \leq i < j \leq N} K_{00}(Q_i \cdots Q_{j-1})}, \tag{4.32}$$

then using (4.14) we get

$$\begin{aligned} \hat{K}_{R_1 \dots R_N}^{(m)}(Q_1, \dots, Q_{N-1}) &= M(q, R_i) \\ &\prod_{i=1}^N \mathcal{W}_{R_i}^2 \prod_{1 \leq i < j < N-1} (1 - q^k Q_i \dots Q_{j-1})^{-C_k(R_i, R_j)} \\ &\prod_{i=1}^N (1 - q^k Q_i \dots Q_{N-1})^{-C_k(R_i, R_N)}. \end{aligned}$$

The partition function is given by

$$\begin{aligned} \hat{Z}^{(m)} &= \sum_{R_1, \dots, R_N} \left(\prod_{i=1}^N Q_{b_i}^{l_{R_i}} \right) \hat{K}_{R_1 \dots R_N}^{(N-2)}(Q_1, \dots, Q_{N-1}) \hat{K}_{R_1 \dots R_N}^{(m)}(Q_1, \dots, Q_{N-1}) \\ &= \sum_{R_1, \dots, R_N} \left(\prod_{i=1}^N Q_{b_i}^{l_{R_i}} \right) M(q, R_i) \\ &\quad \frac{\prod_{i=1}^N \mathcal{W}_{R_i}(q)^2}{\prod_{1 \leq i < j \leq N} \prod_k (1 - q^k Q_i \dots Q_{j-1})^{2C_k(R_i, R_j^T)}}. \end{aligned} \quad (4.33)$$

In writing the above expression we have changed R_N to R_N^T and absorbed a factor of $q^{-\kappa_N}$ into $M^{(m)}(q, R_i)$. Studying the limits $Q_{F_i} \rightarrow 0$ as in the previous section, we can determine the framing factor to be

$$M^{(m)}(q, R_i) = (-1)^{(N+m)(l_1 + \dots + l_N)} q^{1/2 \sum_{i=1}^N (N+m-2i)\kappa_i}. \quad (4.34)$$

Recall that when $N + m$ is even (odd), the corresponding geometry contains Hirzebruch surfaces \mathbb{F}_{2r} (\mathbb{F}_{2r+1}). The Kähler parameters T_{b_i} are related to the Kähler parameter of the base T_B and of the fibers $T_{F_1, \dots, N-1}$ via,

for $N + m = 2r + 1$,

$$\begin{aligned} T_{b_{r+1}} &= T_B, \\ T_{b_{r+1-i}} &= T_B + \sum_{j=1}^i (2j-1) T_{F_{r+1-j}}, \quad i = 1, \dots, r, \\ T_{b_{r+1+i}} &= T_B + \sum_{j=1}^i (2j-1) T_{F_{r+j}}, \quad i = 1, \dots, N-r-1, \end{aligned} \quad (4.35)$$

and for $N + m = 2r$,

$$\begin{aligned}
T_{b_r} &= T_{b_{r+1}} = T_B, \\
T_{b_{r-i}} &= T_B + \sum_{j=1}^i 2j T_{F_{r-j}}, \quad i = 1, \dots, r-1 \\
T_{b_{r+1+i}} &= T_B + \sum_{j=1}^i 2j T_{F_{r+j}}, \quad i = 1, \dots, N-r-1,
\end{aligned} \tag{4.36}$$

where T_{b_i} is to be set to 0 if $i > N$ or $i < 1$. The above relation between the Kähler parameters is depicted in figure 12. It can be determined from the fact that the divisors which appear in the local geometry are

$$\{\mathbb{F}_{m+2-N}, \mathbb{F}_{m+4-N}, \dots, \mathbb{F}_{m+2r-N}, \dots, \mathbb{F}_{m+N-2}\}, \tag{4.37}$$

where \mathbb{F}_{-n} for $n > 0$ is to indicate that the corresponding subdiagram within the web diagram for the $SU(N)$ geometry occurs upside down as compared to the subdiagram for \mathbb{F}_n .

From (4.37) we can easily determine $\prod_i Q_{b_i}^{l_i}$ to be

$$\prod_{i=1}^N Q_{b_i}^{l_{R_i}} = \begin{cases} Q_B^{\sum_{i=1}^N l_{R_i}} \prod_{i=1}^{(N+m-1)/2} Q_{F_i}^{(N+m-2i)(l_1+\dots+l_i)} \\ \quad \prod_{i=((N+m-1)/2)+1}^{N-1} Q_{F_i}^{(2i-N-m)(l_{i+1}+\dots+l_N)}, & N+m = \text{odd} \\ Q_B^{\sum_{i=1}^N l_{R_i}} \prod_{i=1}^{((N+m)/2)-1} Q_{F_i}^{(N+m-2i)(l_1+\dots+l_i)} \\ \quad \prod_{i=((N+m)/2)+1}^{N-1} Q_{F_i}^{(2i-N-m)(l_{i+1}+\dots+l_N)}, & N+m = \text{even}. \end{cases} \tag{4.38}$$

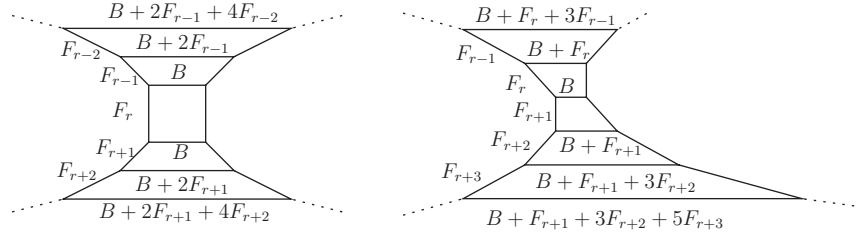


Figure 12: Identifying the Kähler classes of curves, for geometries containing even Hirzebruch surfaces (left) and odd (right).

5 Nekrasov's conjecture and the field theory limit

Ever since the work of Seiberg and Witten [24], it has been a challenge to reproduce their results using instanton calculus. In [13, 14, 17, 18], this calculus is used to express the coefficients \mathcal{F}_k of the k -instanton contributions to the prepotential as integrals over the moduli space of instantons which can be evaluated using localization techniques. These calculations become feasible when the integral localizes to a finite number of points. In [10], this was achieved by a certain deformation of the integrand by parameters ϵ_1 and ϵ_2 . While the $\epsilon_{1,2} \rightarrow 0$ limit cannot be taken in the individual integrals $Z_k(\epsilon_1, \epsilon_2)$, [10] assembles these into an infinite sum

$$\mathcal{Z}(\varphi, \epsilon_1, \epsilon_2) = 1 + \sum_{k=1}^{\infty} Z_k(\epsilon_1, \epsilon_2) \varphi^k, \quad (5.1)$$

from which a generating function $\mathcal{F}(\varphi, \epsilon_1, \epsilon_2) = \sum_{k=1}^{\infty} \mathcal{F}_k(\epsilon_1, \epsilon_2) \varphi^k$ can be extracted via

$$\mathcal{Z} = \exp\left(-\frac{1}{\epsilon_1 \epsilon_2} \mathcal{F}\right), \quad (5.2)$$

such that $\lim_{\epsilon_{1,2} \rightarrow 0} \mathcal{F}_k(\epsilon_1, \epsilon_2) = \mathcal{F}_k$. Somewhat surprisingly, \mathcal{Z} has physical significance at finite $\epsilon_1 = -\epsilon_2 = \hbar^7$ as well. For this choice of parameters, [10] derives the following result (in our notation)

$$\mathcal{Z} = \sum_{R_1, \dots, R_N} \varphi^{l_{R_1} + \dots + l_{R_N}} \prod_{l,n=1}^N \prod_{i,j=1}^{\infty} \frac{a_{ln} + \hbar(\mu_{l,i} - \mu_{n,i} + j - i)}{a_{ln} + \hbar(j - i)}. \quad (5.3)$$

The sum over R_1, \dots, R_N runs over Young tableaux, as there is a 1 : 1 correspondence between an ordered N -tuple of Young tableaux and the points at which the deformed integrals localize. As conjectured in [10] and shown in [19], in the case of $SU(2)$, this expression reproduces the field theory limit of the topological string partition function, for a particular choice of fibration of the resolved A_n geometry over \mathbb{P}^1 , with the parameter \hbar acquiring the role of the string coupling.

In [10], it was further conjectured that the following simple modification of this expression in fact reproduces the *complete* string partition function,

$$Z_{\text{Nekrasov}} := \sum_{R_1, \dots, R_N} \varphi^{l_{R_1} + \dots + l_{R_N}} \prod_{l,n=1}^N \prod_{i,j=1}^{\infty} \frac{\sinh[\beta(a_{ln} + \hbar(\mu_{l,i} - \mu_{n,i} + j - i))/2]}{\sinh[\beta(a_{ln} + \hbar(j - i))/2]}. \quad (5.4)$$

This conjecture was also verified, again in the $SU(2)$ case, in [19].

⁷ \hbar , following Nekrasov's notation, denotes an arbitrary constant.

In this section, we wish to extend the verification of Nekrasov's conjecture to the general $SU(N)$ case. The calculation goes through almost exactly as in the $SU(2)$ case.

In [19], we noted that using the definition of $\mathcal{W}_R(q)$ and the following identity

$$\prod_{1 \leq i < j < \infty} \frac{[\mu_i - \mu_j + j - i]}{[j - i]} = \prod_{1 \leq i < j \leq d(\mu)} \frac{[\mu_i - \mu_j + j - i]}{[j - i]} \prod_{i=1}^{d(\mu)} \prod_{v=1}^{\mu_i} \frac{1}{[v - i + d(\mu)]}, \quad (5.5)$$

we have, with $q = e^{-\beta \hbar}$,

$$\mathcal{W}_R^2(q) = 2^{-2l_R} q^{\kappa_R/2} \prod_{i,j=1}^{\infty} \frac{\sinh[\beta \hbar(\mu_i - \mu_j + j - i)/2]}{\sinh[\beta \hbar(j - i)/2]}. \quad (5.6)$$

Furthermore,

$$\prod_k (1 - q^k Q)^{-2C_k(R_r, R_s^T)} = Q^{-l_{R_r} - l_{R_s}} 2^{-2(l_{R_r} + l_{R_s})} q^{-1/2(\kappa_{R_r} - \kappa_{R_s})} \prod_{l \neq n, i, j} \frac{\sinh[\beta(a_{ln} + \hbar(\mu_{l,i} - \mu_{n,j} + j - i))/2]}{\sinh[\beta(a_{ln} + \hbar(j - i))/2]}, \quad (5.7)$$

where $l, n \in \{r, s\}$, $i, j \geq 1$, $Q = e^{-\beta a_{r,s}}$. The above two identities imply, using $\sum_{i < j} (\kappa_i - \kappa_j) = \sum_{i=1}^N (N - 2i + 1) \kappa_i$,

$$\begin{aligned} \hat{Z}^{(m)} &= \sum_{R_1, \dots, R_N} \prod_{i=1}^N Q_{b_i}^{l_{R_i}} M^{(m)}(q, R_i) 2^{-2N(l_1 + \dots + l_N)} \\ &\quad \prod_{i=1}^{N-1} Q_i^{-(N-i)(l_1 + \dots + l_i) - i(l_{i+1} + \dots + l_N)} q^{-1/2 \sum_{i=1}^N (N-2i) \kappa_i} \\ &\quad \prod_{l, n, i, j} \frac{\sinh[\beta(a_{ln} + \hbar(\mu_{l,i} - \mu_{n,j} + j - i))/2]}{\sinh[\beta(a_{ln} + \hbar(j - i))/2]}. \end{aligned} \quad (5.8)$$

Using (5.1) and (4.34), we see that for $m = 0$,

$$\hat{Z}^{(0)} = \sum_{R_1, \dots, R_N} \varphi^{l_1 + \dots + l_N} \prod_{l, n, i, j} \frac{\sinh[\beta(a_{ln} + \hbar(\mu_{l,i} - \mu_{n,j} + j - i))/2]}{\sinh[\beta(a_{ln} + \hbar(j - i))/2]}, \quad (5.9)$$

where

$$\varphi = \frac{Q_B}{2^{2N} D(Q_{F_i})},$$

$$D(Q_{F_i}) = \begin{cases} \prod_{i=1}^{N-1/2} Q_{F_i}^i \prod_{i=(N-1/2)+1}^{N-1} Q_{F_i}^{N-i}, & N = \text{odd} \\ \prod_{i=1}^{N/2-1} Q_{F_i}^i \prod_{i=N/2+1}^{N-1} Q_{F_i}^{N-i}, & N = \text{even.} \end{cases}$$

Taking the field theory limit

$$Q_B = (-1)^{N-m} \left(\frac{\beta\Lambda}{2}\right)^{2N}, \quad Q_{F_j} = e^{-\beta a_{j,j+1}}, \quad \beta \rightarrow 0, \quad (5.10)$$

we get

$$\mathcal{Z}^{(m)} = \sum_{R_{1,\dots,N}} \left(\frac{\Lambda}{2}\right)^{2N(l_1+\dots+l_N)} \prod_{l,n,i,j} \frac{a_{ln} + \hbar(\mu_{l,i} - \mu_{n,j} + j - i)}{a_{ln} + \hbar(j - i)}. \quad (5.11)$$

Evaluating the sum above upto representations of combined length k yields, by invoking (5.2), the instanton coefficients \mathcal{F}_k of $\mathcal{N} = 2$ $SU(N)$ gauge theory. This evaluation is performed in equations (3.23) and (3.24) of [10], and the results coincide with previous work employing Seiberg–Witten techniques [25].

Acknowledgments

A.I. would like to thank Marcos Mariño and Cumrun Vafa for valuable discussions. The research of A.I. was supported by NSF award NSF-DMS/00-74329. The research of A.K. was supported by the Department of Energy under contract number DE-AC03-76SF00515.

Appendix A

$SU(N)$ Geometries

In this section, we would like to sketch the origins of the diagrams encoding the A_{n-1} fibrations over \mathbb{P}^1 that we study in this paper. While not self contained, we hope that we will give the reader with a passing familiarity with toric geometry a clearer understanding of how these diagrams arise.

A_{n-1} singularities are of the form $\mathbb{C}^2/\mathbb{Z}_n$. The corresponding toric diagram is depicted in figure A.1.

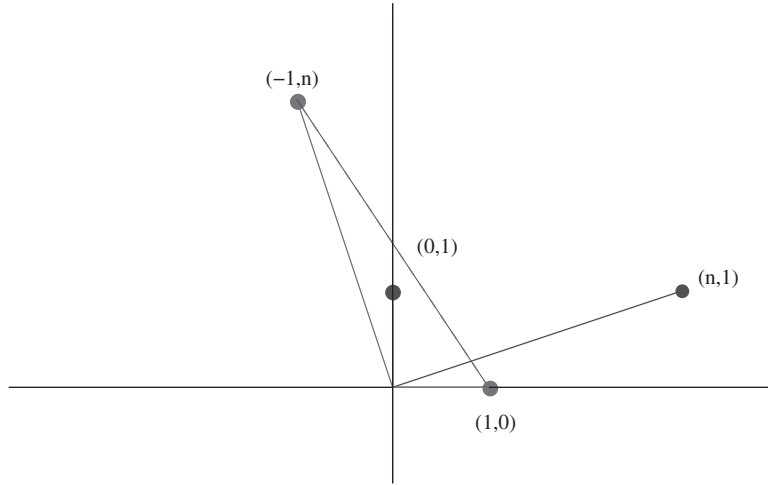


Figure A.1: The fan for A_{n-1} (in blue) and its dual fan (in red).

We can read off the coordinate ring of the toric variety from the dual fan. It is given by

$$\mathbb{C} \left[x, \frac{y^n}{x}, y \right] = \mathbb{C}[a, b, c]/(ab - c^n), \quad (\text{A.1})$$

which we recognize as the coordinate ring of $\mathbb{C}^2/\mathbb{Z}_n$. The fact that the corresponding variety is singular is encoded in the toric diagram in the fact that the single 2-cone comprising the fan is not generated by (part of) a basis of the lattice: rather than being generated by maximally two vectors, the fan is generated by the $n + 1$ vectors $\{(1, 0), (1, 1), \dots, (n, 1)\}$. Subdividing the fan as depicted in figure A.2 yields the toric diagram for the resolution of the A_{n-1} singularity.

We now want to fiber these geometries over \mathbb{P}^1 , the toric diagram of which is depicted in figure A.3.

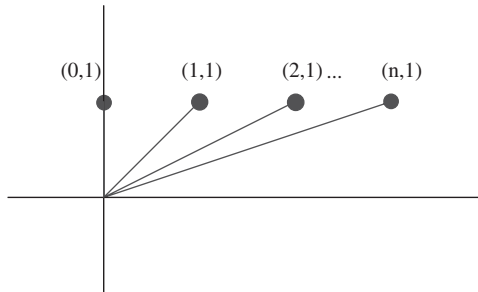


Figure A.2: The resolved A_{n-1} geometry.



Figure A.3: The fan for \mathbb{P}^1 .

To this end, we embed figure A.2 in a three-dimensional lattice. To preserve the Calabi–Yau condition, we only add cones which are generated by vectors ending on the plane through the point $(0, 1, 0)$ and parallel to the xz plane. In the diagrams in figure A.4, we omit the y direction. Adding any two cones such that their projection onto the z -axis yields the toric diagram of \mathbb{P}^1 yields the desired geometry. The specific choice of cones determines how the resolved A_{n-1} singularity is fibered over the \mathbb{P}^1 .

In figure A.4, we present the fans for fibrations of resolved A_2 over \mathbb{P}^1 , and the corresponding web diagrams. Note that this comprises all possible choices. If we move the vector $(a, 1)$ further to the right than the $(2, 1)$ position that yields the geometry with divisor \mathbb{F}_2 and \mathbb{F}_4 , we obtain a space with more than two compact divisors. This is evident e.g., from the fact that the external legs of the web diagram start crossing past this point. On the other hand, if we move the vector further to the left than the $(-1, 0)$ position of the $\mathbb{F}_1 - \mathbb{F}_1$ geometry, we reproduce fibrations already considered.

The considerations for the general case are completely analogous. Note that the web diagrams can also be obtained by gluing together the web

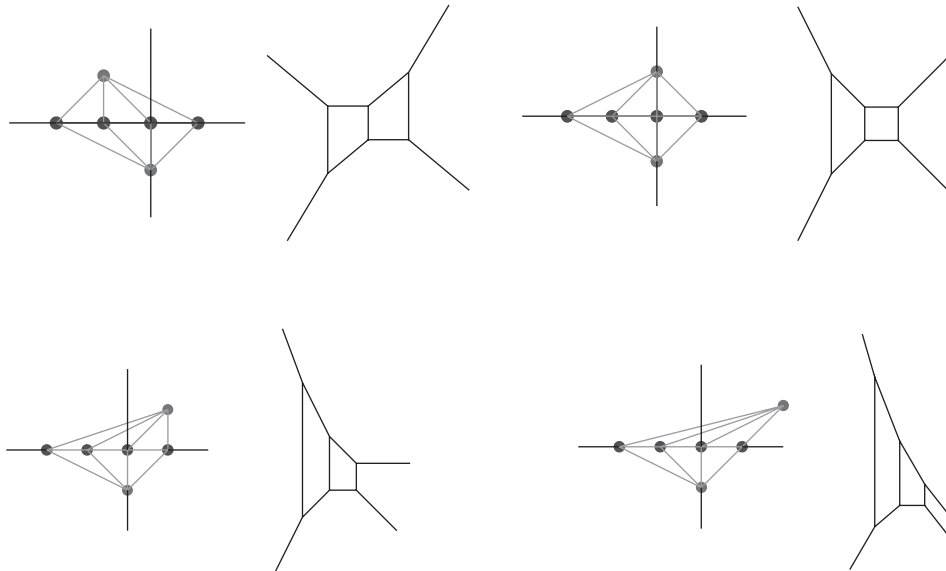


Figure A.4: A_2 fibrations over \mathbb{P}^1 .

diagrams of local Hirzebruch surfaces \mathbb{F}_k , where the k 's of adjacent surfaces differ by 2. We label the fibrations by an integer m , where $m = N$ denotes the geometry with the sequence $\{\mathbb{F}_2, \mathbb{F}_4, \dots\}$ of divisors, and count downwards. For the case $N = 2$, this reproduces the conventional labeling for Hirzebruch surfaces.

$SU(N)$ geometries and the 5d Chern–Simons coefficient

The label m we use to distinguish the various fibrations for a given N is related to the triple intersection number of divisors and as such has a physical significance in the 5d theory one obtains by considering M-theory compactification, instead of type IIA, on the CY3-folds we have been considering [26, 27]. The five-dimensional theory has a prepotential with a cubic term. This cubic term arises from the Chern–Simons term $\text{Tr}(A \wedge F \wedge F)$, where A is the gauge field and F its field strength, in the corresponding Lagrangian. The coefficient of this term, with appropriate normalization, is an integer called the Chern–Simons coefficient. From the CY point of view, the cubic term in the prepotential arises from the triple intersection numbers as follows [27, 28]. Let $S_i(m)$ be the various divisors which in our case are either even or odd Hirzebruch surfaces depending on $N + m$ even or odd,

$$S_i(m) \in \{\mathbb{F}_{m+2-N}, \mathbb{F}_{m+4-N}, \dots, \mathbb{F}_{m+2r-N}, \dots, \mathbb{F}_{m+N-2}\}. \quad (\text{A.2})$$

Define $S(m) = \sum_{i=1}^{N-1} (\phi_{i+1} + \dots + \phi_N) S_i$, where ϕ_i , in the 5d theory, parametrize the Coulomb branch moduli space. Then,

$$S^3 = \sum_{i,j,k} (\phi_{i+1} + \dots + \phi_N)(\phi_{j+1} + \dots + \phi_N)(\phi_k + \dots + \phi_N) (S_i \cdot S_j \cdot S_k) \quad (\text{A.3})$$

is such that

$$S^3(m) = \frac{1}{2} \sum_{i,j} |\phi_i - \phi_j|^3 + m \sum_i \phi_i^3. \quad (\text{A.4})$$

Thus the term we are using to label the geometries is exactly the Chern–Simons coefficient of the 5d theory.

References

- [1] C. Vafa, *Superstrings and topological strings at large N*, J. Math. Phys. **42** (2001) 2798–2817, hep-th/0008142.

- [2] M. Aganagic, M. Mariño and C. Vafa, *All loop topological string amplitudes from Chern–Simons theory*, hep-th/0206164.
- [3] D.-E. Diaconescu, B. Florea and A. Grassi, *Geometric transitions and open string instantons*, hep-th/0205234; *Geometric transitions, del Pezzo surfaces and open string instantons*, hep-th/0206163.
- [4] A. Iqbal, *All genus topological string amplitudes and 5-brane webs as Feynman diagrams*, hep-th/0207114.
- [5] M. Aganagic, M. Marino, A. Klemm and C. Vafa, *The topological vertex*, hep-th/0305132.
- [6] A. Klemm, W. Lerche, P. Mayr, C. Vafa and N.P. Warner, *Self-dual strings and $N = 2$ supersymmetric field theory*, Nucl. Phys. B **477**(746) (1996), arXiv:hep-th/9604034.
- [7] S. Katz, A. Klemm and C. Vafa, *Geometrical engineering of quantum field theories*, Nucl. Phys. **B497** (1997), 196–204, hep-th/9609239.
- [8] A. Klemm, W. Lerche, P. Mayr, C. Vafa and N. Warner, *Self-dual strings and $N = 2$ supersymmetric field theory*, Nucl. Phys. **B477** (1996), 746–766, hep-th/9604034.
- [9] S. Katz, P. Mayr and C. Vafa, *Mirror symmetry and exact solution of 4D $N = 2$ gauge theories. I*, Adv. Theor. Math. Phys. **1**(53) (1998), arXiv:hep-th/9706110.
- [10] N. Nekrasov, *Seiberg–Witten prepotential from instanton counting*, hep-th/0206161.
- [11] R. Flume and R. Poghossian, *An algorithm for the microscopic evaluation of the coefficients of the Seiberg–Witten prepotential*, hep-th/0208176.
- [12] U. Bruzzo, F. Fucito, J.F. Morales and A. Tanzini, *Multi-instanton calculus and equivariant cohomology*, arXiv:hep-th/0211108.
- [13] N. Dorey, V.V. Khoze and M.P. Mattis, *Multi-instanton calculus in $N = 2$ supersymmetric gauge theory*, Phys. Rev. **D54** (1996), 2921–2943, hep-th/9603136.
- [14] N. Dorey, V.V. Khoze and M.P. Mattis, *Multi-instanton calculus in $N = 2$ supersymmetric gauge theory. II: Coupling to matter*, Phys. Rev. **D 54**(7832) (1996), arXiv:hep-th/9607202.
- [15] D. Bellisai, F. Fucito, A. Tanzini and G. Travaglini, *Multi-instantons, supersymmetry and topological field theories*, Phys. Lett. B **480**(365) (2000), arXiv:hep-th/0002110.
- [16] D. Bellisai, F. Fucito, A. Tanzini and G. Travaglini, *Instanton calculus, topological field theories and $N = 2$ super Yang–Mills theories*, JHEP **0007**(017) (2000), arXiv:hep-th/0003272.

- [17] R. Flume, R. Poghossian and H. Storch, *The Seiberg–Witten prepotential and the Euler class of the reduced moduli space of instantons*, Mod. Phys. Lett. A **17(327)** (2002), arXiv:hep-th/0112211.
- [18] T.J. Hollowood, *Calculating the prepotential by localization on the moduli space of instantons*, JHEP **0203(038)** (2002), arXiv:hep-th/0201075.
- [19] A. Iqbal and A.-K. Kashani-Poor, *Instanton counting and Chern–Simons theory*, hep-th/0212279.
- [20] R. Gopakumar and C. Vafa, *M-theory and topological strings-I*, hep-th/9809187; *M-theory and topological strings-II*, hep-th/9812127.
- [21] E. Witten, *Chern–Simons gauge theory as a string theory*, in The Floer Memorial Volume; Birkhäuser, 1995, p. 637, hep-th/9207094.
- [22] M. Mariño, *Enumerative geometry and knot invariants*, hep-th/0210145.
- [23] H. Ooguri and C. Vafa, *Worldsheet derivation of a large N duality*, Nucl. Phys. **B641** (2002), 3–34, hep-th/0205297.
- [24] N. Seiberg and E. Witten, *Monopole condensation, and confinement in $N = 2$ supersymmetric Yang–Mills theory*, Nucl. Phys. **B426** (1994), 19–52, hep-th/9407087; *Monopole, duality and chiral symmetry breaking in $N = 2$ supersymmetric QCD*, Nucl. Phys. **B431** (1994), 484–550, hep-th/9408099.
- [25] E. D’Hoker, I.M. Krichever and D.H. Phong, *The effective prepotential of $N = 2$ supersymmetric $SU(N(c))$ gauge theories*, Nucl. Phys. B **489(179)** (1997), arXiv:hep-th/9609041.
- [26] N. Seiberg, *Five dimensional SUSY field theories, non-trivial fixed points and string dynamics*, hep-th/9608111; *Webs of (p,q) 5-branes, five dimensional field theories and grid diagrams*, hep-th/9710116.
- [27] K.A. Intriligator, D.R. Morrison and N. Seiberg, *Five-dimensional supersymmetric gauge theories and degenerations of Calabi–Yau spaces*, Nucl. Phys. B **497(56)** (1997), arXiv:hep-th/9702198.
- [28] A. Iqbal and V.S. Kaplunovsky, *Quantum deconstruction of a 5D SYM and its moduli space*, arXiv:hep-th/0212098.